

Nickel and helium evidence for melt above the core–mantle boundary

Claude Herzberg¹, Paul D. Asimow², Dmitri A. Ionov^{3,4}, Chris Vidito¹, Matthew G. Jackson⁵ & Dennis Geist⁶

High ³He/⁴He ratios in some basalts have generally been interpreted as originating in an incompletely degassed lower-mantle source^{1–9}. This helium source may have been isolated at the core–mantle boundary region since Earth's accretion^{4–6}. Alternatively, it may have taken part in whole-mantle convection and crust production over the age of the Earth^{7–9}; if so, it is now either a primitive refugium at the core–mantle boundary⁸ or is distributed throughout the lower mantle^{7,9}. Here we constrain the problem using lavas from Baffin Island, West Greenland, the Ontong Java Plateau, Isla Gorgona and Fernandina (Galapagos). Olivine phenocryst compositions show that these lavas originated from a peridotite source that was about 20 per cent higher in nickel content than in the modern mid-ocean-ridge basalt source. Where data are available, these lavas also have high ³He/⁴He. We propose that a less-degassed nickel-rich source formed by core–mantle interaction during the crystallization of a melt-rich layer or basal magma ocean^{5,6}, and that this source continues to be sampled by mantle plumes. The spatial distribution of this source may be constrained by nickel partitioning experiments at the pressures of the core–mantle boundary.

Primitive mantle has been estimated to contain 1,960 p.p.m. nickel (Ni)¹⁰, and this is similar to estimates for depleted peridotite¹¹, which makes up the average mid-ocean-ridge basalt (MORB) source. It is also similar to the Ni content of fertile peridotite (which has less basalt than primitive peridotite but more melt than depleted peridotite so more basalt can be extracted during partial melting) obtained from recent high-quality measurements¹² (Supplementary Fig. 1 and Supplementary section 1), which can be described by:

$$\text{Ni (p.p.m.)} = 68.6\text{MgO (weight per cent)} - 630 \quad (1)$$

Equation (1) fits the Ni contents of 110 fertile and depleted peridotite compositions to 92 p.p.m. ($\pm 2\sigma$); we refer to this as normal Ni peridotite. High-precision olivine analyses from these fertile and depleted peridotites¹² yield 2,800–3,100 p.p.m. Ni and magnesium (Mg)-numbers of 89–92 (that is, 100MgO/(MgO + FeO) in mole per cent; Fig. 1a, Supplementary Table 1 and Supplementary Information section 2). These olivines from mantle peridotite are very similar to primitive olivine phenocryst compositions from East Pacific Rise (EPR) basalts (Fig. 1a). They are also very similar to model Ni contents¹³ shown by the black line in Fig. 1, which is appropriate for olivine phenocrysts of primary magmas having 8%–38% MgO and for melting of both fertile and depleted upper-mantle peridotite. Model olivines are also similar to observed olivine phenocrysts in hot Archaean komatiites from Alexo^{14,15} (Fig. 1b) and other occurrences of high-temperature magmas (Methods), demonstrating restricted compositions over a broad temperature range¹³.

Olivines from the Palaeocene-epoch picrites in Baffin Island and West Greenland, on the other hand, have higher Ni contents (up to

3,800 p.p.m.) than those from MORBs, Archaean komatiites, and mantle peridotite (Fig. 1c). Those with high Mg-numbers are also higher in Ni than olivines that are expected to crystallize from any partial melt of normal mantle peridotite, as indicated by Ca, Mn and Fe/Mn (Fig. 2). Primary magma major-element compositions were estimated from modelling of whole-rock lava compositions¹⁶, but sorting of olivine phenocrysts in lava flows compromises reliable Ni estimates with this method. However, the Ni contents and Mg-numbers of the olivine phenocrysts themselves are unaffected by crystal sorting. We estimated a typical Ni content of the primary magma that is required to crystallize olivines with the observed Ni and highest Mg-numbers. The high-Ni olivines require a fertile peridotite source having $\sim 2,360$ p.p.m. Ni (Methods Summary). This is about 20% higher than normal Ni peridotite with 1,960 p.p.m. Ni and is well outside the 2σ uncertainty bounds of equation (1). The range of olivine compositions at low Mg-numbers and Ni contents is a consequence of variable olivine and clinopyroxene fractionation from primary magmas (Fig. 1c and Supplementary Information section 4).

The excess-Ni problem is not confined to Baffin Island and West Greenland. Although high-precision Ni data for olivine in intraplate occurrences are limited, we find high Ni in olivines from the Ontong Java plateau, Gorgona komatiites, and the Fernandina volcano in the Galapagos islands (Fig. 3). In all cases a peridotite source provenance is indicated by Ca, Mn and Fe/Mn (refs 13, 14) in olivine (Fig. 2 and Supplementary Information). The high Ni in Gorgona olivines is clearly seen because the sample suite includes olivines with very high Mg-numbers, close to those expected for early crystals from the primary magmas. The high Ni in olivines from the other occurrences is less clear, owing to their lower Mg-numbers. For these we modelled the Ni contents of olivines that would crystallize from primary magmas and their liquid lines of descent. Using primary magma compositions from ref. 16 with the Ni contents adjusted to those expected in melts from normal fertile peridotite containing 1,960 p.p.m. Ni (Fig. 1), the Ni contents of olivines that crystallize along liquid lines of descent are always lower than those observed in olivines from the Ontong Java plateau or the Fernandina volcano, regardless of the proportions of crystallizing olivine and clinopyroxene. Rather, all successful solutions require Ni-rich fertile peridotite sources having Ni contents up to 2,360 p.p.m.

Mantle that has been depleted by prior melting events can be high in both MgO and NiO compared with more fertile sources (see equation (1)). However, the Ni contents of partial melts of highly depleted peridotite and fertile peridotites are indistinguishable at liquid MgO < 25 weight per cent¹³ (Supplementary Fig. 1) and the olivines of primary melts shown in Fig. 1c should be generally applicable. Therefore, Ni-rich olivine phenocrysts cannot crystallize from melts of normal depleted peridotite.

Excess Ni in olivine has also been attributed to high temperatures and pressures of melting¹⁷. However, this is not consistent with olivines

¹Department of Earth and Planetary Sciences, Rutgers University, 610 Taylor Road, Piscataway, New Jersey 08854-8066, USA. ²Geological and Planetary Sciences, California Institute of Technology, Pasadena, California 91125, USA. ³Département de Géologie, Université J. Monnet (member of PRES Université de Lyon), 23 rue P. Michelon, 42023 Saint-Etienne Cedex 2, France. ⁴Laboratoire Magmas et Volcans, CNRS UMR 6524, 42023 Saint Etienne, France. ⁵Department of Earth and Environment, Boston University, 685 Commonwealth Avenue, Boston, Massachusetts 02215, USA. ⁶Department of Geological Sciences, University of Idaho 3022, Moscow, Idaho 83844, USA.

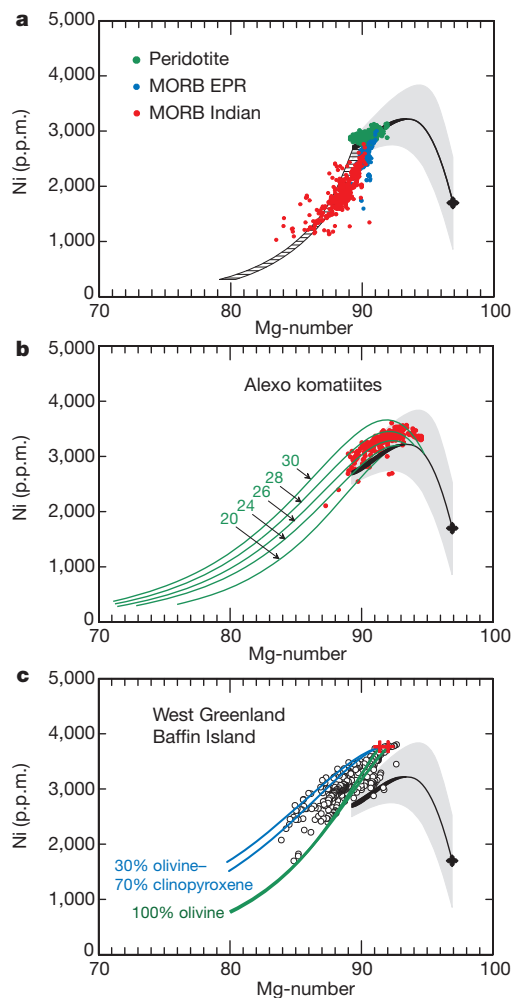


Figure 1 | Mg-numbers and Ni content for calculated¹³ and observed olivine. An Mg-number is defined as $100\text{MgO}/(\text{MgO} + \text{FeO})$ in mole per cent. The black curve represents the calculated Ni content in olivines that crystallize from all primary melts derived from a fertile peridotite source having a whole-rock Ni content of 1,960 p.p.m. (ref. 13); the $\pm 1\sigma$ uncertainty (grey shading) is discussed in Supplementary Information section 3. The black hatched area represents the calculated Ni content in olivines from olivine-fractionated derivative liquids from primary magmas having 8–13% MgO. **a**, The green circles are 203 high-precision analyses of olivine in mantle peridotite from various tectonic settings (Supplementary Information); the blue and red circles are high-precision olivine phenocrysts in MORBs from the Pacific (the EPR) and Indian oceans^{14,17}. **b**, The red circles are high-precision olivine phenocrysts from the Archaean Alexo komatiites¹⁴. The green curves are calculated Ni contents in olivines from olivine-fractionated derivative liquids from primary magmas having 20–30% MgO (ref. 13), as indicated (green numbers); primary magmas for Alexo contained 26–30% MgO (refs 13, 15). **c**, The white circles are high-precision olivine phenocrysts from West Greenland and Baffin Island¹⁴; the uncertainty is only slightly greater than the size of the open circles. The red crosses are the Ni contents of olivine phenocrysts expected to crystallize from primary melts derived from Ni-rich fertile peridotite having 2,360 p.p.m. Ni. The green and blue lines are olivine compositions that will crystallize from these primary magmas by fractionation of olivine and clinopyroxene in the weight proportions indicated (Supplementary Information). A low-Ni population comes from one sample (ID 27142) from West Greenland¹⁴, and it represents 28% of the database, having Mg-number > 90. There is little overlap between this sample and the more Ni-rich types. The difference between the low- and high-Ni populations most probably reflects mantle source heterogeneity, but there are no independent geochemical data for these samples with which to test this possibility.

from Archaean komatiites from Alexo¹⁴ (Fig. 1b) and Barberton (see Methods), which are thought to be among the hottest magmas ever erupted on Earth¹⁵, and yet have normal Ni concentrations. Appealing

to the formation of Alexo komatiites in a cool and wet environment does not solve the problem because they are compositionally similar to komatiites from the Belingwe greenstone belt¹⁸ for which melt inclusion studies point to a hot and dry origin¹⁹. Furthermore, Barberton komatiites separated from a deep garnet-bearing residue that was hot and dry, and yet there is no excess Ni (Methods); low-temperature hydrous melting models are also not consistent with olivine phenocryst compositions (Methods). Consequently, the high Ni contents of the Baffin Island and West Greenland olivines are more plausibly related to composition rather than temperature-pressure effects.

Shield volcanoes from Hawaii also contain olivine phenocrysts with increased Ni (refs 14, 17), and there is general agreement that Hawaii is melting from a source that is hotter than the ambient mantle^{16,17}. High Ni contents in Hawaiian olivines have been used to infer both pyroxenite melting in the source^{13,14} and high temperatures and pressures of peridotite melting¹⁷. Comparably high mantle potential temperatures have been inferred for both Hawaii and West Greenland occurrences (1,500–1,600 °C; ref. 16) and both erupted through thick lithosphere (Supplementary Information). If increased temperature and pressure is the main mechanism for producing olivine phenocrysts with high Ni contents¹⁷, there should be similar Ni, Mn, Fe/Mn and Ca contents in olivines from Hawaii and from Baffin Island and West Greenland. This is not observed (Supplementary Fig. 8). Hawaiian olivines are higher in Ni by $\sim 1,000$ p.p.m. and they have substantially lower calcium (Ca) and manganese (Mn) and higher Fe/Mn contents than those from West Greenland and Baffin Island. For the latter, a peridotite source provenance is clearly indicated (Fig. 2 and Supplementary Fig. 8). By contrast, low Ca and low Mn and high Fe/Mn contents for Hawaiian olivines are an expected consequence of pyroxenite source melting, owing to residuum retention of Ca in clinopyroxene and Mn in garnet (Supplementary Fig. 5). It is pyroxenite that contributes to high Ni in Hawaiian olivines^{13,14}, not temperature and pressure effects¹⁷. However, a possible role for mixed Ni-rich and Ni-poor peridotite with pyroxenite remains to be evaluated for Hawaii.

We conclude that high Ni coupled to peridotite-generated levels of Ca, Mn and Fe/Mn (Figs 1–3 and Supplementary Figs 6 and 7) point to Ni-rich peridotite sources for Baffin Island, West Greenland, Ontong Java plateau, Isla Gorgona and Fernandina in the Galapagos islands. By ‘Ni-rich’, we refer to Ni contents that are significantly higher than those described by equation (1), in contrast with normal-Ni peridotite sources that melt to make modern oceanic crust at mid-ocean ridges (Fig. 1a).

Current estimates of the Ni content of fertile mantle peridotite^{10,11} are based on averages which can vary by about 300 p.p.m. (ref. 13); the Ni content of olivine in such peridotites obtained from open-access web sources is also large¹⁷. Although our estimated Ni content for Ni-rich peridotite is roughly within this range, we emphasize that this coincidence has no meaning because whole-rock and olivine Ni data are often compiled from sources of questionable accuracy¹³, and there is much less uncertainty in our more recent work¹² (Fig. 1 and Supplementary Fig. 1). Random ± 300 p.p.m. variations in the Ni content of peridotite can result in olivines with Ni as low as 2,200 p.p.m. (ref. 13). Such low Ni contents have never been reported from high-precision olivine analyses in unmetasomatized mantle peridotite (Fig. 1a) and, when found in olivine phenocrysts¹⁴, other explanations are more plausible. For example, some MORB olivines can be low in Ni (Fig. 1a), but this is plausibly explained by sequestration of Ni into a residual sulphide phase¹³, which can remain stable in the residue up to 15% melting²⁰.

Lavas exhibiting Ni excess are also associated with elevated $^3\text{He}/^4\text{He}$. Picrites from Baffin Island and West Greenland have $^3\text{He}/^4\text{He}$ up to 50 times the atmospheric value (Ra) (ref. 21), and they also have primitive Nd and Pb isotopic compositions³. For the others, the maximum $^3\text{He}/^4\text{He}$ (Ra) is 29 for Fernandina² and 18 for Gorgona²². No helium data are currently available for lavas from the Ontong Java plateau, but they also have primitive Nd and Pb isotopic ratios⁸.

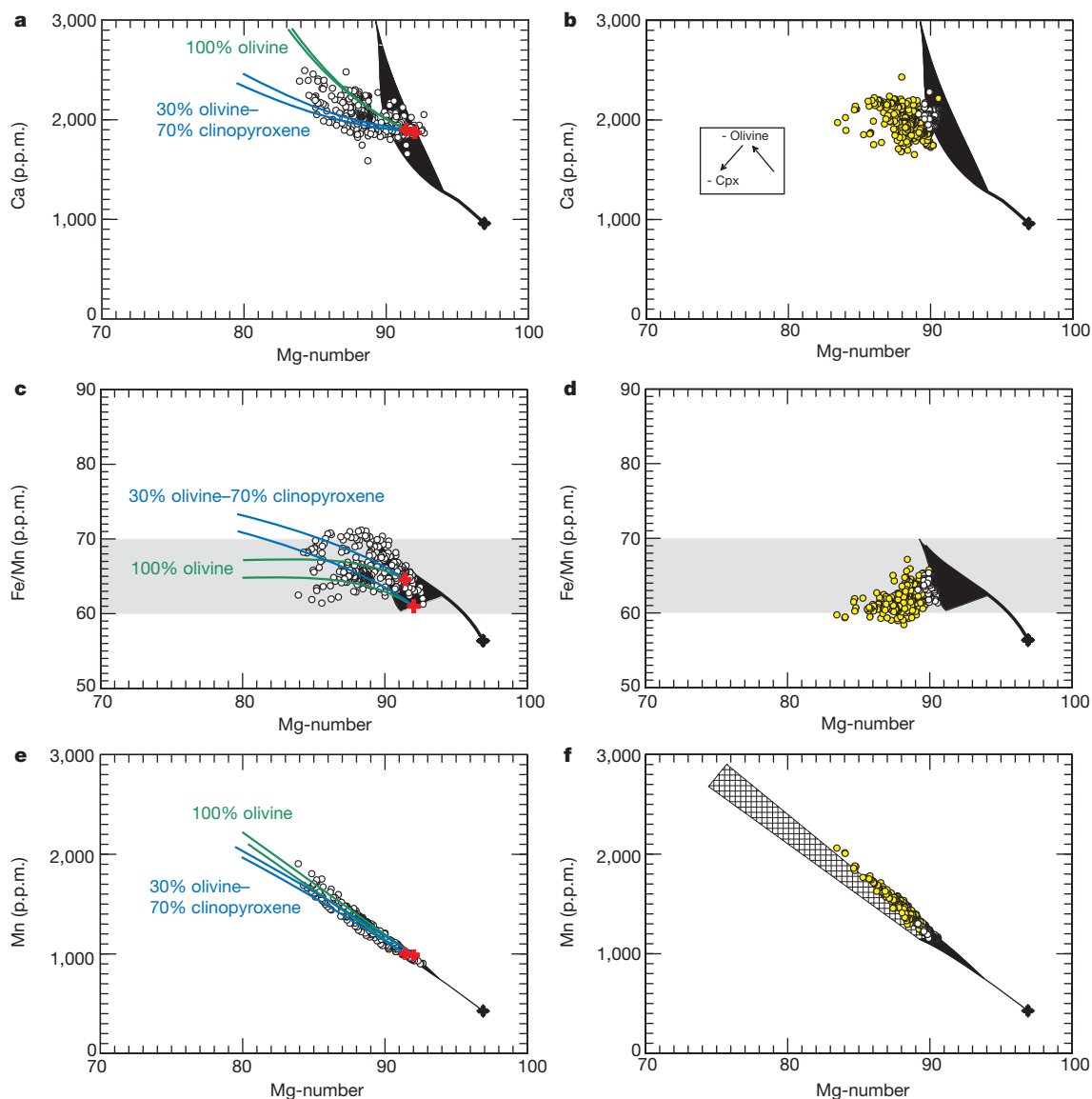


Figure 2 | Mg-numbers and Ca, Mn and Fe/Mn contents for calculated¹³ and observed olivine phenocrysts from MORBs (right panels) compared with Baffin Island and West Greenland¹⁴ (left panels). The black regions are calculated olivines from primary melts (8–38% MgO) derived by peridotite melting¹³. The black hatched area in f and the grey shading in c and d represent the calculated olivines from olivine-fractionated derivative liquids from primary magmas having 8–20% MgO. The green and blue lines in a, c and e are olivine compositions that crystallize from primary magmas that fractionated olivine and clinopyroxene in the weight proportions indicated (Supplementary

We now explore a model that might produce a Ni-rich peridotite with increased ³He/⁴He. We have tested the formation of Ni-rich peridotite in a magma ocean by perovskite subtraction and/or ferropericlase addition. Although such models can yield high Ni contents, they produce a peridotite source that is too low in SiO₂ and Fe/Mn that is too high. More work on intra-mantle differentiation scenarios informed by accurate high-pressure phase equilibria and partitioning data are warranted⁶, but here we propose a core–mantle interaction model.

Evidence for melting at the present-day core–mantle boundary includes the coincidence of recent determinations of the peridotite solidus with the estimated temperature at the top of the outer core²³ and seismic observations of ultralow-velocity zones²⁴. As even more melt is expected in an early hotter Earth, present-day ultralow-velocity zones may represent the terminal stages in the crystallization of a long-lived magma ocean, and they provide a possible mechanism for

Information). The inset in b shows how Ca in olivine changes owing to olivine and clinopyroxene fractionation from the primary magmas. The MORBs in b, d and f are from the EPR (white circles) and Indian Ocean (yellow circles). Although a wide range of Ca contents are theoretically possible for olivines that crystallize from peridotite-source primary magmas, most have ~2,000 p.p.m. Ca—similar to those found in MORBs, Baffin Island and West Greenland. Primitive and depleted peridotites contain ~1,000 p.p.m. Mn (refs 10, 11) and, although olivines with Fe/Mn = 55–70 can crystallize from primary magmas, more usually the range is restricted to 60–65 (ref. 13).

preserving primitive mantle^{5,6}. This model predicts an equilibrium exchange of Ni between liquid metal in the core and liquid silicate in the mantle, which can be described by^{25–27}:



The present-day Ni content of fertile mantle peridotite (~1,960 p.p.m.) may have been established by core formation at ~30–60 GPa (ref. 25 and references therein). Silicate melt in contact with liquid metal would be enriched in Ni at 135 GPa as the exchange is driven from left to right with increasing pressure at constant oxidation state of iron^{25–27}. We propose that a Ni-rich and less-degassed domain was formed by core–mantle interaction during the late stages of the crystallization of a basal magma ocean⁵ or melt layer, and that some part of this source continues to be sampled by mantle plumes. Another

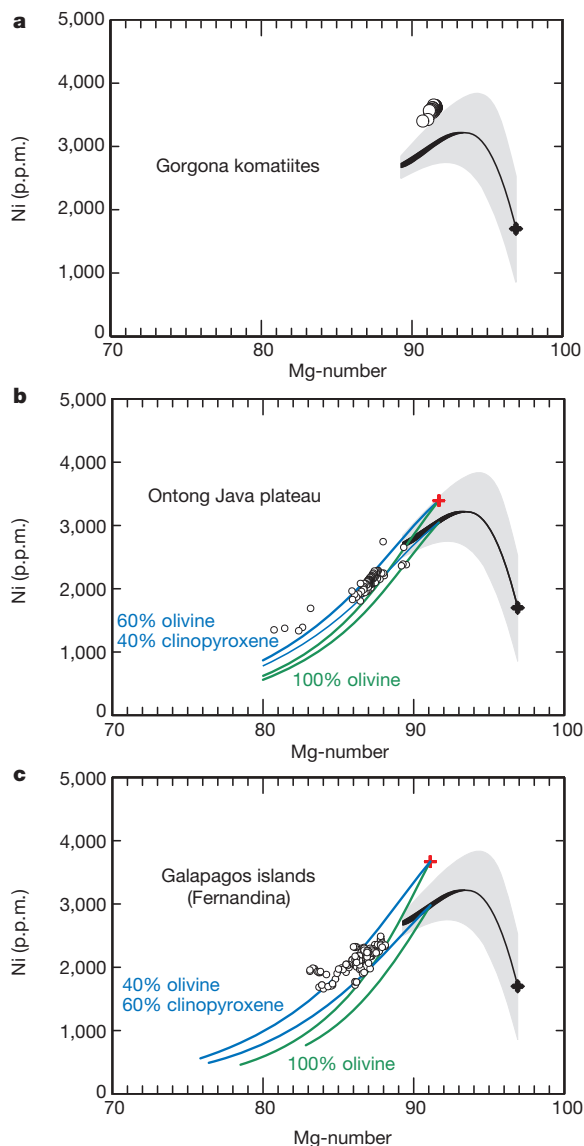


Figure 3 | Mg-numbers and Ni contents for calculated olivine¹³ and observed olivine phenocrysts. **a**, Gorgona¹⁴, **b**, the Ontong Java Plateau¹⁴, and **c**, Fernandina (this work; Supplementary Information section 5 and Supplementary Table 2). The black curves represent the calculated Ni content in olivines of primary magmas of fertile peridotite having 1,960 p.p.m. Ni (ref. 13); the grey shaded regions ($\pm 1\sigma$) represent a possible range of Ni contents in olivine that may arise from uncertainties in the calculation (Supplementary Information). The red crosses are olivines that would crystallize from Ni-rich fertile peridotite-source primary magmas; the green and blue lines are olivine compositions that crystallize from primary magmas that fractionated olivine and clinopyroxene in the weight proportions indicated (Supplementary Information section 4).

tracer for core–mantle interaction may be the addition of tungsten and osmium (Os) isotopes from the core to the mantle^{27,28}. Gorgona is the only location examined here with available ¹⁸⁶Os/¹⁸⁸Os data, and there is an ¹⁸⁶Os anomaly that has been attributed to core influence²⁸. There is no shortage of plausible mechanisms of core–mantle interaction, and the challenge is to understand how they are geochemically expressed²⁷.

Earth's mantle may have become oxidized by disproportionation of FeO in a deep magma ocean during crystallization of Fe³⁺-rich Mg-perovskite and loss of metallic Fe to the core²⁹. The Ni-rich peridotite source for West Greenland is also oxidized, having produced melts more oxidizing than MORB and within one log unit of the

nickel–nickel oxide oxygen fugacity buffer³⁰. Although it is counter-intuitive, we propose that these oxidized magmas had an origin that began above the core–mantle boundary, in a location where Ni-rich silicate melt and Fe³⁺-rich Mg-perovskite were in equilibrium with the outer core. Mantle plumes that sample this region and ascend above the melting zone would solidify to Ni-rich ferroprecipitate, Ca perovskite and Fe³⁺-rich Mg-perovskite, transforming further to Ni-rich and oxidized peridotite in the upper mantle. Partial melting will yield magmas like those from West Greenland that are both Ni-rich and more oxidizing than MORB.

The spatial distribution of elevated ³He/⁴He in the mantle might be constrained by understanding the origin of a Baffin Island and West Greenland source with 2,360 p.p.m. Ni. Although core formation in a single stage is not likely²⁶, its prediction of 3,580 p.p.m. Ni (ref. 26) in the mantle at 135 GPa may be a guide to the Ni content of silicate melt at the present time. A source with 2,360 p.p.m. Ni would then require mixing of this high-Ni endmember with the canonical ~1,960 p.p.m. Ni from elsewhere in the mantle. In this scenario, the Ni-rich and high-³He/⁴He source may be widely distributed^{7,9} or it may take the form of a halo around the core. Alternatively, the isolation of the Baffin Island and West Greenland source as a refuge from convection near the core–mantle boundary^{4–6,8} is plausible if it can be demonstrated that 2,360 p.p.m. Ni in a silicate melt is in equilibrium with the core. In any case, interaction of the core with a silicate melt is a plausible mechanism for production of oxidized Ni-rich peridotite, and it provides evidence for a long-lived melt layer or basal magma ocean^{5,6}.

METHODS SUMMARY

The method for calculating model olivine Ni compositions is given elsewhere¹³ and in the Supplementary Information. Primary magma compositions are calculated first, followed by the olivines that they crystallize.

The compositions of Ni in liquids extracted from dunite [liquid + olivine] and harzburgite [liquid + olivine + orthopyroxene] residues were computed by mass-balance solutions to the equation for accumulated fractional melting:

$$C_L = C_o[1 - (1 - F)^{1/D}]/F$$

where C_L is weight per cent NiO in the liquid (primary magma), C_o is the initial NiO in the peridotite source composition (0.25%, ref. 10; 1,960 p.p.m.), F is the melt fraction, and D is the bulk distribution coefficient from the Beattie–Jones model (Supplementary Information). Ni contents for near-solidus melts were calculated from the MgO contents of near-solidus melts, together with a solidus olivine composition having 0.36% NiO (ref. 13) (Supplementary Information). Ni contents of near-solidus primary magmas are nearly indistinguishable from those of primary magmas for liquid + olivine and liquid + olivine + orthopyroxene assemblages, and the full range of possible Ni contents are shown in Supplementary Fig. 1.

The Ni content of olivine that crystallizes as a phenocryst at one atmosphere from a primary magma C_L was calculated using olivine/liquid Ni distribution coefficients from the Beattie–Jones model (Supplementary Information). Results are displayed in Figs 1 and 3 for a fertile peridotite having $C_o = 1,960$ p.p.m. Ni. Olivines have 2,800–3,100 p.p.m. Ni, and they provide an excellent description of olivine in normal mantle peridotite, primitive olivine phenocrysts in modern MORB, and olivine phenocrysts in Archean komatiites. However, they fail to describe the much higher Ni contents of olivines from Baffin Island, West Greenland, the Ontong Java Plateau, Isla Gorgona and Fernandina (Galapagos) (Figs 1c and 3). For these, excellent agreement between computed and observed olivine Ni contents could be obtained with $C_o = 0.30\%$ NiO (2,360 p.p.m. Ni), a Ni-rich peridotite source.

Full Methods and any associated references are available in the online version of the paper.

Received 10 May; accepted 5 November 2012.

Published online 9 January 2013.

1. Kurz, M. D., Jenkins, W. J. & Hart, S. R. Helium isotopic systematics of oceanic islands and mantle heterogeneity. *Nature* **297**, 43–47 (1982).

2. Kurz, M. D., Curtice, J., Fornari, D., Geist, D. & Moreira, M. Primitive neon from the center of the Galapagos hotspot. *Earth Planet. Sci. Lett.* **286**, 23–34 (2009).
3. Jackson, M. G. *et al.* Evidence for the survival of the oldest terrestrial mantle reservoir. *Nature* **466**, 853–856 (2010).
4. Tolstikhin, I. & Hofmann, A. W. Early crust on top of the Earth's core. *Phys. Earth Planet. Inter.* **148**, 109–130 (2005).
5. Labrosse, S., Hernlund, J. W. & Coltice, N. A crystallizing dense magma ocean at the base of the Earth's mantle. *Nature* **450**, 866–869 (2007).
6. Coltice, N., Moreira, M., Hernlund, J. & Labrosse, S. Crystallization of a basal magma ocean recorded by helium and neon. *Earth Planet. Sci. Lett.* **308**, 193–199 (2011).
7. Glass, C. & Goldstein, S. L. Evolution of helium isotopes in the Earth's mantle. *Nature* **436**, 1107–1112 (2005).
8. Jackson, M. G. & Carlson, R. W. An ancient recipe for flood-basalt genesis. *Nature* **476**, 316–319 (2011).
9. Gonnermann, H. M. & Mukhopadhyay, S. Preserving noble gases in a convecting mantle. *Nature* **459**, 560–563 (2009).
10. McDonough, W. F. & Sun, S.-s. The composition of the Earth. *Chem. Geol.* **120**, 223–253 (1995).
11. Salters, V. J. M. & Stracke, A. Composition of depleted mantle. *Geochem. Geophys. Geosyst.* **5**, Q05B07 (2004).
12. Ionov, D. A. Compositional variations and heterogeneity in fertile lithospheric mantle: peridotite xenoliths in basalts from Tariat, Mongolia. *Contrib. Mineral. Petrol.* **154**, 455–477 (2007).
13. Herzberg, C. Identification of source lithology in the Hawaiian and Canary islands: implications for origins. *J. Petrol.* **52**, 113–146 (2011).
14. Sobolev, A. V. *et al.* The amount of recycled crust in sources of mantle-derived melts. *Science* **316**, 412–417 (2007).
15. Arndt, N. T., Leshner, C. M. & Barnes, S. J. *Komatiite* 363–389 (Cambridge Univ. Press, 2008).
16. Herzberg, C. & Gazel, E. Petrological evidence for secular cooling in mantle plumes. *Nature* **458**, 619–622 (2009).
17. Putirka, K., Ryerson, F. J., Perfit, M. & Ridley, W. I. Mineralogy and composition of the oceanic mantle. *J. Petrol.* **52**, 279–313 (2011).
18. Puchtel, I. S., Walker, R. J., Brandon, A. D. & Nisbet, E. G. Pt–Re–Os and Sm–Nd isotope and HSE and REE systematics of the 2.7 Ga Belingwe and Abitibi komatiites. *Geochim. Cosmochim. Acta* **73**, 6367–6389 (2009).
19. Berry, A. J., Danyushevsky, D. V., O'Neill, H., St C., Newville, M. & Sutton, S. R. Oxidation state of iron in komatiitic melt inclusions indicates hot Archaean mantle. *Nature* **455**, 960–963 (2008).
20. Bézous, A., Lorand, J.-P., Humler, E. & Gros, M. Platinum-group element systematic in mid-oceanic ridge basaltic glasses from the Pacific, Atlantic, and Indian oceans. *Geochim. Cosmochim. Acta* **69**, 2613–2627 (2005).
21. Starkey, N. A. *et al.* Helium isotopes in early Iceland plume picrites: constraints on the composition of high $^3\text{He}/^4\text{He}$ mantle. *Earth Planet. Sci. Lett.* **277**, 91–100 (2009).
22. Révillon, S. *et al.* Heterogeneity of the Caribbean plateau mantle source: new constraints from Sr, O, and He isotope compositions of olivine and clinopyroxene. *Earth Planet. Sci. Lett.* **205**, 91–106 (2002).
23. Fiquet, G. *et al.* Melting of peridotite to 140 gigapascals. *Science* **329**, 1516–1518 (2010).
24. Williams, Q. & Garnero, E. J. Seismic evidence for partial melt at the base of Earth's mantle. *Science* **273**, 1528–1530 (1996).
25. Siebert, J., Badro, J., Antonangeli, D. & Ryerson, F. J. Metal-silicate partitioning of Ni and Co in a deep magma ocean. *Earth Planet. Sci. Lett.* **321/322**, 189–197 (2012).
26. Rubie, D. *et al.* Heterogeneous accretion, composition, and core-mantle differentiation of the Earth. *Earth Planet. Sci. Lett.* **301**, 31–42 (2011).
27. Walker, D. Core-mantle chemical issues. *Can. Mineral.* **43**, 1553–1564 (2005).
28. Brandon, A. D. *et al.* ^{186}Os – ^{187}Os systematic of Gorgona Island komatiites: implications for early growth of the inner core. *Earth Planet. Sci. Lett.* **206**, 411–426 (2003).
29. Wade, J. & Wood, B. J. Core formation and the oxidation state of the Earth. *Earth Planet. Sci. Lett.* **236**, 78–95 (2005).
30. Larsen, L. M. & Pedersen, A. K. Processes in high-Mg, high T magmas: evidence from olivine, chromite and glass in Paleogene picrites from West Greenland. *J. Petrol.* **41**, 1071–1098 (2000).

Supplementary Information is available in the online version of the paper.

Acknowledgements C.H. thanks L. Larsen, M. Portnyagin, A. Sobolev and D. Walker for discussions. We are very grateful to R. Walker for a critical review. D.A.I. acknowledges PNP grants from the French INSU-CNRS in 2010–2012 and P.D.A. acknowledges NSF grant EAR-1119522. P.D.A. thanks A. Matzen for extended discussions. D.G.'s work is funded by NSF grant EAR1145271.

Author Contributions C.H. modelled olivine compositions and developed a variety of magma ocean and core–mantle interaction interpretations. P.D.A. suggested the core–mantle interaction model in its current form and critiqued all Ni partition models. D.A.I. provided high-precision olivine and whole-rock analyses for mantle peridotite. C.V. acquired high-precision olivine data for Fernandina (Galapagos). M.G.J. provided information on Pb, Nd and He isotopes. D.G. provided rock samples from Fernandina. All authors contributed to the intellectual growth of this paper.

Author Information Reprints and permissions information is available at www.nature.com/reprints. The authors declare no competing financial interests. Readers are welcome to comment on the online version of the paper. Correspondence and requests for materials should be addressed to C.H. (herzberg@rci.rutgers.edu).

METHODS

Our conclusion about a Ni-rich peridotite source is based on our use of the Beattie–Jones model^{31,32} for the partitioning of Ni between olivine and liquid. We adopted it because it provides the minimum error when recovering experimental data compared with other published methods (Supplementary Information).

Putirka *et al.*¹⁷ and Matzen *et al.*³³ argued that it is the temperature difference ΔT between separation from a high-pressure residue and onset of crystallization at shallower depths that accounts for the high Ni contents of olivine for Hawaii. This is termed a ΔT model. If this were true then it might be argued that this ΔT model is an alternative explanation to that of an Ni-rich peridotite source for Baffin Island, West Greenland, the Ontong Java Plateau, Isla Gorgona and Fernandina. However, the ΔT model of Putirka *et al.*¹⁷ is based on a parameterization of experimental data with much larger errors than the Beattie–Jones Ni partitioning model (Supplementary Fig. 3 and Supplementary Information). We cannot comment on the ΔT model of Matzen *et al.*³³ because has not yet been published. Nevertheless, we examine in more detail the ΔT model because of its potential to compromise our interpretations.

Major-element, trace-element and isotope evidence suggest that the Barberton komatiites separated from a dry garnet-bearing peridotite residue at pressures in excess of 8 GPa (refs 34–38). The temperature difference between source and eruption conditions is about 300 °C for Barberton (see figure 5 in ref. 39), and about 150 °C for Hawaii^{17,39}. The ΔT model predicts higher Ni contents of olivines in Barberton komatiites than in Hawaii. However, just the opposite is observed. Primitive Barberton olivines are lower in Ni than Hawaiian examples by more than 1,000 p.p.m. Ni (refs 36, 40) (Supplementary Figs 8 and 11; A. V. Sobolev, personal communication, 2012). This paradox might be resolved if the Barberton komatiites formed by low-temperature wet melting in a subduction environment^{40–42} rather than dry hot melting in mantle plumes^{34–39}. In this model melting is extensive: it goes beyond garnet stability, leaving behind a harzburgite residue. However, it is problematic because it ignores the aggregate body of evidence for residual garnet in heavy rare earth element depletions^{36,38}, CaO/Al₂O₃ and absolute major-element abundances^{34,35}, and positive ϵ_{Hf} together with subchondritic Lu/Hf³⁷.

The wet melting model is also not consistent with Barberton olivine compositions from the Komati Formation. Barberton olivines have Ca contents that are similar to olivines that crystallize from primary and derivative magmas of dry peridotite^{36,40} (Supplementary Fig. 11). Previous calculations of Ca contents were based on accumulated fractional melting¹³, but batch melting may have played a part at some stage owing to high melt densities at pressures above 8 GPa (refs 34, 36). Accordingly, olivines were computed from dry 7-GPa garnet-bearing melting experiments³⁵, and some are similar to olivines reported by ref. 40. The Ca contents of Barberton komatiites are consistent with melting that was hot, dry and deep, a conclusion that holds for either accumulated fractional melting or batch melting (Supplementary Fig. 11).

Experimental data show that the effect of magmatic H₂O is substantially to lower the Ca contents of olivines^{43–45} (Supplementary Fig. 12), and it has been estimated that there was 5.4% to 7.1% magmatic H₂O for Barberton komatiite production^{42,43}. If it is true that Barberton komatiites had ~6% magmatic H₂O

then this amount would be expected to drop the Ca content of olivine by ~1,000 p.p.m. relative to the dry system (Supplementary Fig. 12). Tenner *et al.*⁴⁵ drew attention to the possible relevance of their wet melting experiments on peridotite KLB-1 to the wet melting model for komatiites, and the MgO contents of their experimental melts (19%–27%) are roughly similar to the 23% MgO used in refs 40 and 41. However, a magmatic H₂O content of 6% is expected to crystallize olivines with ~1,000 p.p.m. Ca (Supplementary Fig. 12), in contrast to observed Barberton olivine phenocrysts, which average ~1,800 p.p.m. Ca (Supplementary Fig. 11). We conclude that the evidence for wet melting is weak and that Barberton komatiites separated from a deep garnet-bearing residue that was hot and dry. Normal Ni contents of Barberton olivines simply reflect the melting of a normal peridotite source. More complex models invoking temperature and pressure effects^{17,33} are not consistent with olivine phenocryst compositions for Barberton komatiites.

- Beattie, P. Ford, C. & Russell, D. Partition coefficients for olivine-melt and orthopyroxene-melt systems. *Contrib. Mineral. Petrol.* **109**, 212–224 (1991).
- Jones, J. H. Temperature and pressure-independent correlations of olivine-liquid partition coefficients and their application to trace element partitioning. *Contrib. Mineral. Petrol.* **88**, 126–132 (1984).
- Matzen, A. K., Baker, M. B., Beckett, J. R. & Stolper, E. M. Ni partitioning between olivine and high-MgO silicate melts: implications for Ni contents of forsteritic phenocrysts in basalts. *Abstr. Goldschmidt Conf.* <http://www.vmgoldschmidt.org/2012/> (2012).
- Herzberg, C. Geodynamic information in peridotite petrology. *J. Petrol.* **45**, 2507–2530 (2004).
- Walter, M. J. Melting of garnet peridotite and the origin of komatiite and depleted lithosphere. *J. Petrol.* **39**, 29–60 (1998).
- Robin-Popieul, C. C. M. *et al.* A new model for Barberton komatiites: deep critical melting with high melt retention. *J. Petrol.* **53** (11), 2191–2229 (2012).
- Blichert-Toft, J., Arndt, N. T. & Gruau, G. Hf isotopic measurements on Barberton komatiites: effects of incomplete sample dissolution and importance for primary and secondary signatures. *Chem. Geol.* **207**, 261–275 (2004).
- Corgne, A. *et al.* Trace element partitioning between majoritic garnet and silicate melt at 10–17 GPa: implications for deep mantle processes. *Lithos* **148**, 128–141 (2012).
- Herzberg, C., Condie, K. & Korenaga, J. Thermal history of the Earth and its petrological expression. *Earth Planet. Sci. Lett.* **292**, 79–88 (2010).
- Parman, S. W., Dann, J. C., Grove, T. L. & de Wit, M. J. Emplacement conditions of komatiite magmas from the 3.49 Ga Komati Formation, Barberton Greenstone Belt, South Africa. *Earth Planet. Sci. Lett.* **150**, 303–323 (1997).
- Grove, T. L. & Parman, S. W. Thermal evolution of the Earth as recorded by komatiites. *Earth Planet. Sci. Lett.* **219**, 173–187 (2004).
- Grove, T. L., Parman, S. W. & Dann, J. C. in *Mantle Petrology: Field Observations and High Pressure Experimentation: A Tribute to Francis R. (Joe) Boyd* (eds Fei, Y., Bertka, C. M. & Mysen, B. O.) 155–167 (The Geochemical Society, Special Publication 6, 1999).
- Parman, S. W. & Grove, T. L. Harzburgite melting with and without H₂O: experimental data and predictive modeling. *J. Geophys. Res.* **109**, B02201 (2004).
- Balta, J. B., Asimow, P. D. & Mosenfelder, J. L. Hydrous, low-carbon melting of garnet peridotite. *J. Petrol.* **52**, 2079–2105 (2011).
- Tenner, T. J., Hirschmann, M. M. & Humayun, M. The effect of H₂O on partial melting of garnet peridotite at 3.5 GPa. *Geochem. Geophys. Geosyst.* **13**, Q03016 (2012).